



Research Article

## Energy, economic and environmental analysis and comparison of the novel Oxy- combustion power systems

Ibrahim OZSARI<sup>1,\*</sup>, Yasin UST<sup>2</sup>

<sup>1</sup>Department of Naval Architecture and Marine Engineering, Bursa Technical University, Yildirim, 16350, Bursa, Turkiye

<sup>2</sup>Department of Naval Architecture and Marine Engineering, Yıldız Technical University, Besiktas, 34349, Istanbul, Turkiye

### ARTICLE INFO

#### Article history

Received: 20 December 2021

Accepted: 22 June 2022

#### Keywords:

Thermodynamic Analysis;  
Oxy-combustion Cycle;  
Gas Turbine; Clean Energy;  
Thermal Efficiency;  
Oxy-fuel/s-CO<sub>2</sub> Cycles

### ABSTRACT

Oxy-combustion technologies are clean energy systems with zero emission; they have great potential when considering global warming and climate change. This study presents a detailed thermodynamic analysis in terms of energy, environment, and economy. Consequently, the results obtained for an oxy-combustion power system are presented in comparison with a conventional gas turbine power system. The results are presented as a function of the pressure ratio with regard to net power, input heat, system efficiency, specific fuel consumption, equivalence ratio, fuel-air ratio, capital investment cost, fuel cost, oxygen cost, total cost, electricity revenue, and net profit. In addition, the study calculates the pollutant emissions from non-oxy-combustion systems and investigates the environmental costs. The pressure ratio for maximum net power has been obtained as 20.8 in the conventional gas turbine power system. Similarly, the pressure ratios for maximum net power in oxy-combustion power cycles with 26%, 28%, and 30% oxygen ratios are 23.3, 27.4 and 29.7, respectively. Results from 24% to 30% have been displayed to observe the effect of reactant oxygen in the oxy-combustion power cycles. The optimum cycle conditions have been determined by calculating the costs of system components, total revenues, and net profits at pressure ratios of 10, 20, 30 and 40. Finally, the results reveal the pressure ratio should be reduced to minimize the total costs per cycle. For maximum net profit, the pressure ratio in a conventional gas turbine power cycle has been calculated as 15.9; similarly, the pressure ratios in oxy-combustion power cycles with 26%, 28%, and 30% oxygen ratios have been respectively calculated as 12.8, 15.2 and 16.4.

**Cite this article as:** Ozsarı I, Ust Y. Energy, economic and environmental analysis and comparison of the novel OXY- combustion power systems. J Ther Eng 2022;8(6):719–733.

\*Corresponding author.

\*E-mail address: Ibrahim.ozsari@btu.edu.tr

This paper was recommended for publication in revised form by Regional Editor

Ahmet Selim Dalkılıç



## INTRODUCTION

With the increasing environmental awareness and global warming crisis in recent years, increasing the penalties and sanctions for harmful emissions has been placed on the agenda, resulting in a concentration of studies on green energy systems. Although numerous investments have been made in renewable energy systems, these have been unable to supply the required energy demand. Therefore, transforming fossil fuel energy systems into environmentally friendly ones is imperative because burning fossil fuels causes harmful emissions such as nitrogen oxides ( $\text{NO}_x$ ) and carbon monoxide (CO) and increases greenhouse gas emissions into the atmosphere. One of the most important technologies that keep the carbon dioxide concentrations resulting from combustion at the desired level is oxy-combustion [1]. Obtaining a flue gas with high carbon dioxide and almost zero nitrogen using oxy-combustion ensures that energy and investment costs in carbon capture and storage technology are significantly reduced and carbon dioxide is easily captured and stored. Different applications are found such as MATIANT, clean energy system (CES), Semi-Closed Oxy-fuel Combustion Combined Cycle (SCOC-CC), NET Power, and GRAZ cycles that are based on oxy combustion. Comparisons of these oxy combustion cycles have been made and their advantages are revealed through numerical data [2,3]. In addition, thermodynamic analysis of oxy-combustion power cycles have been made in many studies [4–7], and suggestions have been presented for making cycles more efficient using various modifications [8,9]. Studies have been presented on the different conditions and parameters regarding the combustion characteristics of oxy-combustion based systems [10–13]. In addition, detailed energy and cost calculations have been made on cycle components such as air separation units (ASUs), combustion chambers, and carbon capture and storage systems [14–20]. In addition, detailed experimental and numerical studies have been carried out on the components of the latest technological energy systems [21–25]. Detailed energy and exergy analyses have been made on the thermodynamic characteristics in oxy-combustion. In addition, a thermodynamic comparison of oxy-combustion and conventional air combustion has also been performed [26].

Scaccabarozzi et al. [27] studied the effects of the Allam cycle on equipment performance for maximum efficiency, optimal cycle parameters, and efficiency. They showed the cooling medium temperature, the power consumption of the air separation unit, the efficiency of the regenerator, and the efficiency of the turbine cooling system to be the main factors affecting cycle efficiency. Thorbergsson and Grönstedt [28] investigated a comparative analysis of two oxy-combustion combined cycles (SCOC-CC and Graz). The Graz cycle has a lower pressure ratio at optimum efficiency and a much higher power density than

SCOC-CC. Khallaghi et al. [29] proposed and evaluated the feasibility of the staged oxy-fuel natural gas combined cycle (SOF-NGCC), which does not require exhaust gas recirculation (EGR). SOF-NGCC is less complex than the Allam cycle and requires smaller equipment. Kotowicz et al. [30] presented a thermodynamic and economic analysis of four variants of the supercritical oxy-combustion power plant using different ASUs and boilers. Shan et al. [31] investigated the effects that different combustion conditions, oxygen concentrations and working conditions such as fuels, different pressures, and working fluids have on the top-blown rotary converter (TBRC) system. They found the optimum pressure of the Brayton cycle to increase with higher concentrations of the combustion oxygen. System efficiency is similar at 21%  $\text{O}_2/\text{N}_2$  conditions and 30%  $\text{O}_2/\text{CO}_2$  conditions. Son et al. [32] designed a new solution by integrating the S- $\text{CO}_2$  oxy-combustion system with concentrated solar energy (CSP). They showed that, using the proposed concept, fuel consumption is reduced by 17–38% compared to traditionally separated systems. Tahir et al. [33] analyzed the characteristics of oxy-fuel combustion in a porous plate reactor. A modified two-step reaction kinetics model was included in the simulation to model methane-air combustion and oxy-fuel combustion. Simulations were made for different oxidizer ratios, mass-flow rates, and reactor heights. The results showed that oxy-combustion with an oxidizer ratio of 0.243 can have the same adiabatic flame temperature as combustion with air. Habib et al. [34] compared and examined the two basic oxy combustion cycles over unmixed combustion conditions and compared their results in terms of exergy destruction and first and second law yields. Wimmer [35] thermodynamically optimized the two high efficiency NET power cycles and the Graz cycle and compared them at full load for demonstrating the oxy-combustion potential. When considering the oxygen supply for the Graz cycle, a slightly higher efficiency was shown at 53.5% compared to 52.7% for the NET power cycle.

This study makes detailed thermodynamic analyses of oxy-combustion power systems using the same system components as a conventional gas turbine power system. The novelty and originality of the study is its detailed comparison of the oxy-combustion power cycle with conventional power plants in terms of energy, environment, and economics. The energy, environmental, and economic results have been examined in detail through the thermodynamic analysis. The results have been evaluated for very significant energy outputs such as net power, input heat, general efficiency, specific fuel consumption, equilibrium ratio, and fuel-air ratio obtained from the system with changes in the pressure ratio. In addition, the economy of initial investment costs, oxygen costs, and fuel costs have been calculated. Oxy combustion's positive environmental impacts have been shown and the harmful emissions and penalties that occur when using conventional gas turbine

power cycle have been calculated. Also, for oxy-combustion power systems, the change in oxygen flow rates during combustion and its effect on energy and economy output have been revealed. As a result, total costs, electricity revenue, and net profits have been calculated for conventional gas turbine power cycle and oxy-combustion power cycles at 26%, 28%, and 30% oxygen ratios. The system components; fuel, environment, and oxygen costs; and net profit results have been presented for four different cycles at 10, 20, 30, and 40 pressure ratios. Thus, all the advantages and disadvantages of the oxy-combustion power cycle are displayed in comparison to conventional power cycles.

### Theoretical Model and Simulation

As seen in Figure 1, conventional gas turbine power system and oxy-combustion power system have common components with compressor, combustion chamber, turbine and regenerator / regenerative heat exchanger. The only different component is a cooler used to separate water in the oxy-combustion power system. While there are many

different combinations of oxy-combustion power cycles, the reason for this simplification is to clearly demonstrate the comparison with thermodynamic analysis. Detailed thermodynamic analyses have been made on the following assumptions;

- All gases are considered ideal and enthalpy and specific heats change with temperature.
- The fuel selected for analyses is natural gas in gaseous form, containing 92.03% CH<sub>4</sub>, 5.75% C<sub>2</sub>H<sub>6</sub>, 1.31% C<sub>3</sub>H<sub>8</sub>, 0.45% C<sub>4</sub>H<sub>10</sub>, 0.46% N<sub>2</sub> [31, 32] and combustion is adiabatic [36,37].
- The air supplied for combustion is completely dry and contains only 0.21 mol O<sub>2</sub> and 0.79 mol N<sub>2</sub>.
- For the unburned air/oxygen and fuel mixture, the reactant temperature is equal to the compressor outlet temperature and the fuel temperature is assumed to be equal to the ambient temperature.
- Combustion is assumed to occur at a steady state and the combustion chamber is assumed a well stirred reactor (WSR) and the primary zone residence time is assumed to be 0.002 seconds.

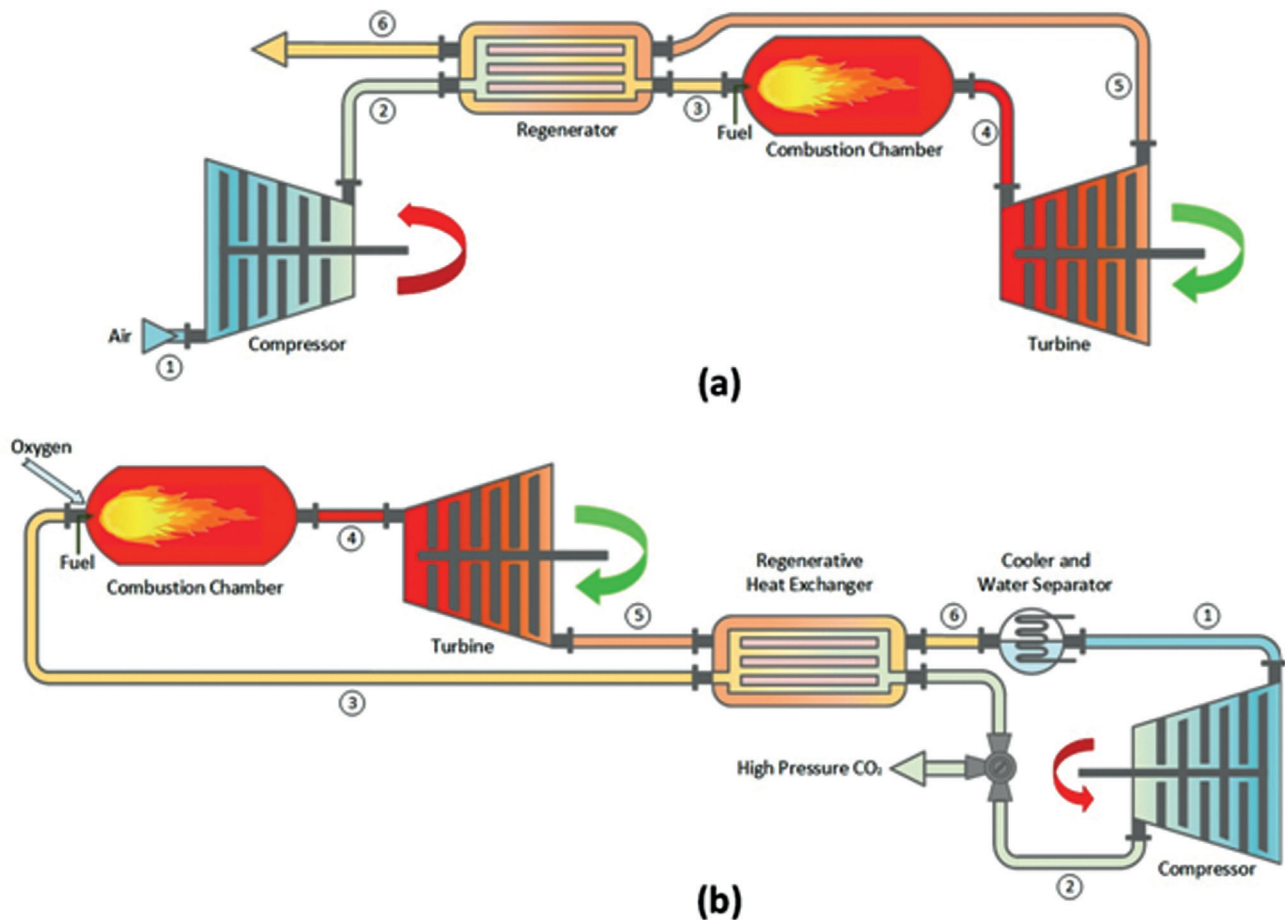


Figure 1. (a) Conventional gas turbine power plant diagram and (b) Oxy-fuel combustion power plant diagram.

- Compressor and turbine efficiency is 88%.
- In the study, the working fluid has a constant mass flow rate and a constant turbine inlet temperature.
- Harmful emission damage costs for CO, NO<sub>x</sub> and CO<sub>2</sub> are taken C<sub>CO</sub> = 0.02086 \$/kg C<sub>NOx</sub> = 6.853 \$/kg CCO<sub>2</sub> = 0.01 \$/kg [38–42].
- Electricity price is taken as C<sub>el</sub> = 0.15 \$ / kWh. [42,43].
- According to Lefebvre, the pressure loss in the combustion chamber varies between 2.5% and 5%. [44]. Therefore, combined pressure loss in the combustion chamber due to friction, turbulence, and temperature rise including the pressure loss in the turbine is assumed to be 4% total.

In order to find the optimum operating performance of the systems, a numerical simulation is prepared in Matlab software. Pressure, temperature, specific heat, enthalpy and entropy values of each component in the plant were calculated in order to compare the conventional gas turbine power plant with the oxy-combustion power plant. Energy equations of energy systems shown in Figure 1 are as follows:

- Compressor

While the compressor outlet temperature changes according to the pressure ratio, the  $k$  values are taken for air and CO<sub>2</sub>, respectively for the conventional gas turbine and the oxy-combustion power systems.

$$T_2 = T_1 \left( 1 + \frac{1}{\eta_c} \left( \text{Pr}^{\frac{k-1}{k}} - 1 \right) \right) \quad (1)$$

$$\dot{W}_C = \dot{m}_{ox} c_p (T_2 - T_1) \quad (2)$$

Calculating the compressor work, the  $c_p$  values are calculated for air and CO<sub>2</sub>.  $C_p$  values change depending on temperature.

$$c_{p,g}(T) = [a_1 + a_2 T + a_3 T^2 + a_4 T^3 + a_5 T^4] R_u \quad (3)$$

- Regenerator/Regenerative Heat Exchanger

$$\dot{m}_{ox}(h_3 - h_2) = \dot{m}_r(h_5 - h_6) \eta_r \quad (4)$$

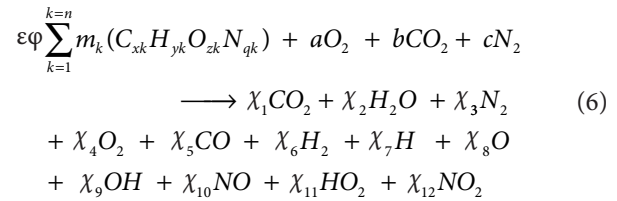
Regenerator pressure loss and efficiency are important for calculation.

$$P_3 / P_2 = (1 - \Delta P_r) \quad (5)$$

- Combustion Chamber

In all gas turbine power cycles, the turbine inlet temperature is constant. The reason for this is the turbine blades can withstand up to a limiting temperature (1400°C) [45]. Also, pressure loss is very important for cycle efficiency. According to [46], preventing 5% pressure loss will be as effective as doubling the compression ratio. The total

pressure loss in the combustion chamber is considered to be 4% regarding turbulence, friction and pressure loss at the turbine inlet. In order to calculate the thermodynamic properties more precisely a combustion model is created. The combustion products are calculated as a function of the equivalence ratio and temperature, taking into account the equilibrium constants. The global chemical equation for the combustion model is as follows:



Here, from  $\chi_1$  to  $\chi_{12}$  represent the number of moles for each species.  $x, y, z, q$  represent the numbers of carbon, hydrogen, oxygen and nitrogen atoms in the fuel, respectively.  $\varphi$  is the overall equivalence ratio.  $\varepsilon$  is the molar air-fuel ratio calculated from stoichiometric combustion of fuel.

$$\varphi = \frac{FA}{FA_s} \quad (7)$$

$$\varepsilon = \frac{4a}{4X + Y - 2Z} \quad (8)$$

The basis of Ferguson's combustion equilibrium method is used to find the 12 unknown mole fractions [47]. Equations (6) and (9) are needed to solve the mole fractions of combustion products. Six of these are provided by the chemical kinetic rates of products. There are four more equations obtained from the atomic balance of the combustion model in the calculation of equilibrium products. Results are obtained numerical method. The system of equations are solved iteratively using Newton Raphson and Gauss Seidel methods. The achievement of the results and their validation with the GASEQ and NASA CEA programs are detailed in the authors' studies [26,48]. These two published publications can be examined for the accuracy of the combustion code. The molar specific heat, enthalpy and entropy values of each type can be obtained from the following expressions by using the curve fitting coefficients ( $a_1 \dots a_n$ ) for the thermodynamic properties of (CHON) systems [49]:

$$\frac{\bar{h}_k}{R_u T} = a_{1,k} + \frac{a_{2,k}}{2} T + \frac{a_{3,k}}{3} T^2 + \frac{a_{4,k}}{4} T^3 + \frac{a_{5,k}}{5} T^4 + \frac{a_{6,k}}{2} \quad (9)$$

$$\frac{\bar{c}_{p,k}}{R_u} = a_{1,k} + a_{2,k} T + a_{3,k} T^2 + a_{4,k} T^3 + a_{5,k} T^4 \quad (10)$$

$$\frac{\bar{s}_k^0}{R_u T} = a_{1,k} \ln T + a_{2,k} T + \frac{a_{3,k}}{2} T^2 + \frac{a_{4,k}}{3} T^3 + \frac{a_{5,k}}{4} T^4 + a_{7,k} \quad (11)$$

At constant pressure, as the mole fractions of the mixture change with temperature, the enthalpy of the mixture changes due to separations. The final specific heat of the gas mixture changes, which is defined as follows:

$$h = \frac{1}{M} \sum_{k=1}^{12} \alpha_k \bar{h}_k [kJ/kg] \quad (12)$$

$$\bar{s} = \frac{R_u}{M} \left[ \sum_{k=1}^n \alpha_k (\bar{s}_k^o - \ln \alpha_k) - \ln \left( \frac{P}{P_0} \right) \right] \quad (13)$$

$$\left( \frac{\partial h}{\partial T} \right)_p = c_{p,g} = \sum_{k=1}^{12} \alpha_k \frac{\partial \bar{h}_k}{\partial T} + \frac{\bar{h}_k}{M} \frac{\partial \alpha_k}{\partial T} - \frac{\alpha_k \bar{h}_k}{M^2} \frac{\partial M}{\partial T} \quad (14)$$

$$\left( \frac{\partial h}{\partial T} \right)_p = c_{p,g} = \frac{1}{M} \left[ \sum_{k=1}^{12} \alpha_k \bar{c}_{p,k} + \bar{h}_k \frac{\partial \alpha_k}{\partial T} - h M_T \right] \quad (15)$$

$$M_T = \frac{\partial M}{\partial T} = \sum_{k=1}^{12} M_k \frac{\partial \alpha_k}{\partial T} \quad (16)$$

Here, the combustion temperature is T (in K). The product molar mass is  $M_k$  and the total products molar mass is M.

$$M = \sum_{k=1}^{12} m_k = \sum_{k=1}^{12} \alpha_k M_k \quad (17)$$

The total number of moles of products can be found by dividing the mass of reactants into the molecular weight of the combustion products as follows: Lastly, the number of moles  $Y_1, Y_2, Y_3 \dots Y_{12}$  are obtained.

$$N = \frac{m_R}{M} \Rightarrow v_k = y_k N \quad (18)$$

To calculate the combustion chamber outlet temperature:

$$T_e = \frac{T_{pz} c_p m_{ox} + T_{cox} c_{p,cox} m_{cox}}{c_p m_{ox} + c_{p,cox} m_{cox}} \quad (19)$$

Here,  $T_{pz}$  is the primary zone air temperature, and  $T_{cox}$  is the dilution air temperature. In addition, the amount of heat generated in the combustion chamber is calculated by the following equation:

$$Q_m = \dot{m}_f LHV / \eta_{cc} \quad (20)$$

• Turbine

$$T_5 = T_4 \left( 1 - \eta_T \left[ 1 - \left( \frac{P_4}{P_5} \right)^{\frac{1-k_g}{k_g}} \right] \right) \quad (21)$$

After obtaining the turbine outlet temperature,  $C_{p,g}$  is obtained from detailed calculation of the gas mixtures entering the turbine after combustion as in equation (3).

$$\dot{W}_T = \dot{m}_T c_{p,g} (T_4 - T_5) \quad (22)$$

$$c_{p,g}(T) = [a_1 + a_2 T + a_3 T^2 + a_4 T^3 + a_5 T^4] R_u \quad (23)$$

Net power is found by subtracting the power generated in turbine from the power consumed in the compressor:

$$\dot{W}_{NET} = \dot{W}_T - \dot{W}_C \quad (23)$$

Specific fuel consumption is calculated from the following equation:

$$SFC = (3600 \dot{m}_f / 1000) / \dot{W}_{NET} [g/kWh] \quad (24)$$

Carbon dioxide and water vapor are products in the stoichiometric combustion of hydrocarbon fuels such as natural gas. In conventional power cycles, less fuel should be burned to reduce emissions of carbon dioxide and water vapor. In oxy-combustion power cycles, water is separated by the cooler and excess carbon dioxide is diverted by a valve mechanism at the compressor outlet for storage. Therefore, the carbon dioxide emissions are calculated depending on the amount of fuel burned for conventional gas turbine power system. [40,41]. Apart from these, two other harmful emissions,  $NO_x$  and CO emissions, are calculated as suggested by [38,44,50–53].  $NO_x$  and CO emissions are obtained as EINO<sub>x</sub> and EICO (grams per kg) using the semi-empirical equations given below. In several studies these semi-empirical formulas are used to calculate  $NO_x$  and CO emissions [39,54,55]. However, it should be noted that unwanted gas emissions are very caustic and specific to operating conditions, so they do not give precise results like OEM warranties in actual engine measurements. Pollutant emissions obtained by thermodynamic simulation analysis are included in the economic calculation as environmental pollution damage cost.

$$\dot{m}_{NO_x} = 0.459 \times 10^{-8} P^{0.25} Ft_{res} \exp(0.01 T_{pz}) \quad (27)$$

$$\dot{m}_{CO} = \frac{0.179 \times 10^9 \exp(7800/T_{pz})}{P^2 t_{res} (\Delta P/P)} \quad (28)$$

Investment, fuel, environmental pollution costs and oxygen costs are calculated required for the oxy-combustion cycle with the following equations to make the total thermo-economic analysis:

$$\dot{C}_{TOT} = \dot{C}_{inv} + \dot{C}_{fuel} + \dot{C}_{env} + \dot{C}_{oxy} \quad (29)$$

$$\dot{C}_{inv} = \sum_{k=1}^n \dot{C}_k \quad [\$ / h] \quad (30)$$

$$\dot{C}_k = \frac{\sum_{k=1}^n C_k CRF \varphi}{N \times 3600} \quad (31)$$

The  $k$  components here represent the cost associated with  $C_k$  capital investment, CRF annual capital recovery factor,  $A$  maintenance factor,  $N$  annual operating hours,  $C_{fuel}$  fuel cost,  $C_{oxy}$  oxygen costs.

$$\sum_{k=1}^n C_k = C_{com} + C_{cc} + C_{tur} + C_{rej/hex} + C_{cool} \quad (32)$$

The purchasing costs of each component in Equation (32) are calculated using the equations in Table 1 used in [56–60].

Fuel, pollutant cost and oxygen cost are calculated with the following equations:

$$\dot{C}_{fuel} = \dot{m}_f c_{fuel} LHV \quad [\$ / h] \quad (33)$$

$$\dot{C}_{env} = \dot{m}_{NO_x} c_{NO_x} + \dot{m}_{CO} c_{CO} + \dot{m}_{CO_2} c_{CO_2} \quad [\$ / h] \quad (34)$$

$$\dot{C}_{oxy} = \dot{m}_{oxy} c_{oxy} \quad [\$ / h] \quad (35)$$

The total cost from the systems electrical energy revenue are subtracted, calculating the net profit:

$$\dot{C}_{PROFIT} = \dot{C}_{SALE} - \dot{C}_{TOT} \quad (36)$$

## RESULTS AND DISCUSSION

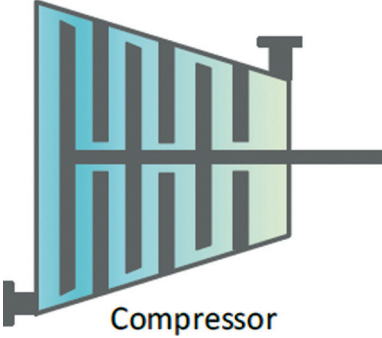

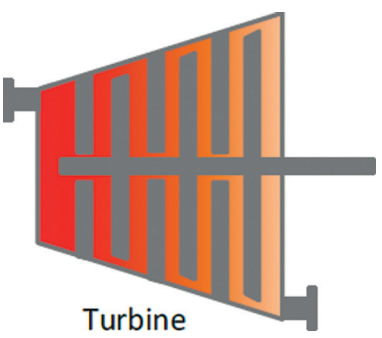
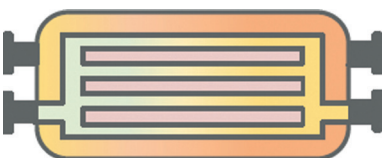

The results from the thermodynamic analyses of conventional gas turbine power system and oxy-combustion power systems in terms of energy, environment, and economy are presented in Figures 2 to 11. Net power, efficiency, input heat, specific fuel consumption, equivalence ratio,

fuel air ratio, harmful emissions and costs, investment costs, fuel costs, total cost, and profit costs have been calculated with respect to various pressure and oxygen ratios, and the results are shown in the figures.

Figures 2a and 2b show the effects changes in pressure and oxygen ratios have on the heat added to the system and net power. As seen in Figure 2a, the net power generated from the system increases rapidly up to 20.8 (PR) in conventional gas turbine power systems. A slight decrease occurs after the peak point of maximum net power. These results are similar in the oxy-combustion power systems. In oxy-combustion power systems, the decrease after the peak point is less than that in conventional gas turbine power systems. The maximum net power obtained in oxy-combustion power systems is 23.3, 27.4 and 29.7 for the peak points in 26%, 28%, and 30% oxy-combustion power systems, respectively. In terms of net power produced, better results are seen to be obtained in conventional gas turbine power systems compared to oxy-combustion power systems for pressure ratios above 10. For pressure ratios between 4 and 10, the 26% oxy-combustion power system is seen to produce more net power. Additionally, conventional gas turbine power systems show better results in terms of heat added the system than the 26% oxy-combustion power at pressure ratios up to 8. Similarly, the conventional gas turbine power system shows better results in terms of heat added the system than the 28% oxy-combustion power at pressure ratios up to 28.3. The 30% oxy-combustion power system always adds less heat to the system than conventional gas turbine combustion. Although the conventional gas turbine power system is more advantageous in terms of power obtained, it is disadvantageous in terms of heat added. As can be seen in Figure 2b, the heat added in the oxy-combustion power cycle is seen to decrease with increases in the pressure and oxygen ratios. The net power obtained by increasing the oxygen ratio in oxy-combustion power systems was determined to decrease. In addition, as the pressure ratio increases from 15 to 30, these decreases are seen to lessen.

Figures 3a and 3b show the effects of changes in pressure and oxygen ratios on system efficiency and specific fuel consumption. As seen in Figure 3a, the overall efficiency of the system increases with increases in the pressure ratio and decreases in the specific fuel consumption. Conventional gas turbine power systems are better than the 28% oxy-combustion power cycle at pressure ratios up to 8. The reason for this is that, although the net power obtained from conventional gas turbine power systems is high, the heat added to the system is also high. The 30% oxy-combustion power cycle up to pressure ratios of 35.3 has the best performance in terms of efficiency. In terms of specific fuel consumption, the conventional gas turbine power system consumes more than the oxy-combustion power systems up to the 9.3 pressure ratio. When the pressure ratio exceeds 33.2, the conventional gas turbine power system has a lower

Table 1. Cost parameters

Components	Investment cost function (\$)	Cost parameters updated to year 2022
 <p>Compressor</p>	$C_{com} = \frac{C_{11}\dot{m}_{ox}}{C_{12} - \eta_c} \left( \frac{P_2}{P_1} \right) \ln \left( \frac{P_2}{P_1} \right)$	$C_{11} = 126.1 \text{ (\$/kg s)}$ $C_{12} = 0.9$
 <p>Combustion Chamber</p>	$C_{cc} = \frac{C_{21}\dot{m}_{ox}}{C_{22} - \left( 1 - \frac{P_4}{P_3} \right)} \left( 1 + e^{C_{23}TIT - C_{24}} \right)$	$C_{21} = 81.27 \text{ (\$/kg s)}$ $C_{22} = 0.995$ $C_{23} = 0.018 \text{ 1/K}$ $C_{24} = 26.4$
 <p>Turbine</p>	$C_{tur} = \left( \frac{C_{31}\dot{m}_T}{C_{32} - \eta_t} \right) \ln \left( \frac{P_4}{P_5} \right) \left( 1 + e^{C_{33}TIT - C_{34}} \right)$	$C_{31} = 845.37 \text{ (\$/kg s)}$ $C_{32} = 0.92$ $C_{33} = 0.036 \text{ 1/K}$ $C_{34} = 54.4$
 <p>Regenerator / Heat Exchanger</p>	$C_{reg} = C_{41} \left( \frac{\dot{Q}_{reg}}{U_{reg} (\Delta T_{LMTD})_{reg}} \right)^{0.6}$	$C_{41} = 7252.1 \text{ (\$/kg s)}$ $U_{reg} = 0.018$
 <p>Cooler and Water Separator</p>	$C_{cool} = C_{51} \left( \frac{\dot{Q}_{cool}}{U_{coll} (\Delta T_{LMTD})_{cool}} \right)^{0.6}$	$C_{51} = 495.58 \text{ (\$/kg s)}$ $U_{cool} = 2.200$

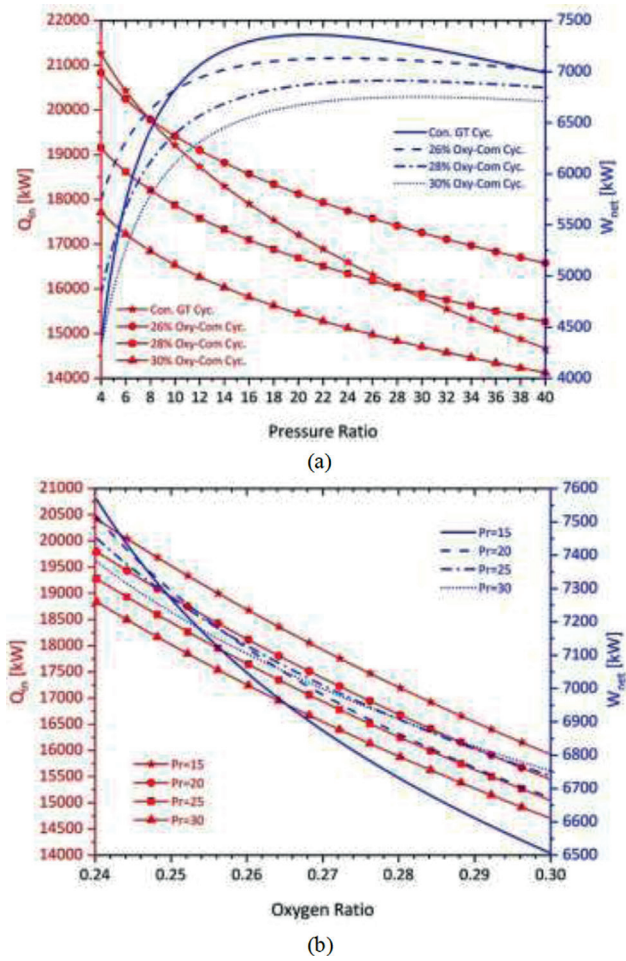


Figure 2. (a) Change of heat added and net power with pressure ratio for various oxygen fractions, (b) Change of heat added and net power with oxygen ratio for various pressure ratio.

specific fuel consumption than the three oxy-combustion power systems. Figure 3b shows the oxy-combustion power cycles efficiency to increase with increases in oxygen and pressure ratios. Also, increasing the oxygen and pressure ratios decreases specific fuel consumption.

As can be seen, Figure 4 demonstrates cycle performances with respect to the net power and efficiency, two important outputs for a system. Thus, power cycles with 26% oxy-combustion are shown to be advantageous in terms of net power. In addition, power cycles with 30% oxy combustion are shown to be more advantageous in terms of efficiency. The general performance map of the systems has been obtained from Figure 4. The power cycle is selected according to the desired output.

Figures 5a and 5b show the effect variations in pressure and oxygen ratios have on the equivalence and fuel-air (FA) ratios. As can be seen in Figure 5a, as the pressure ratio increases in both conventional gas turbine power system

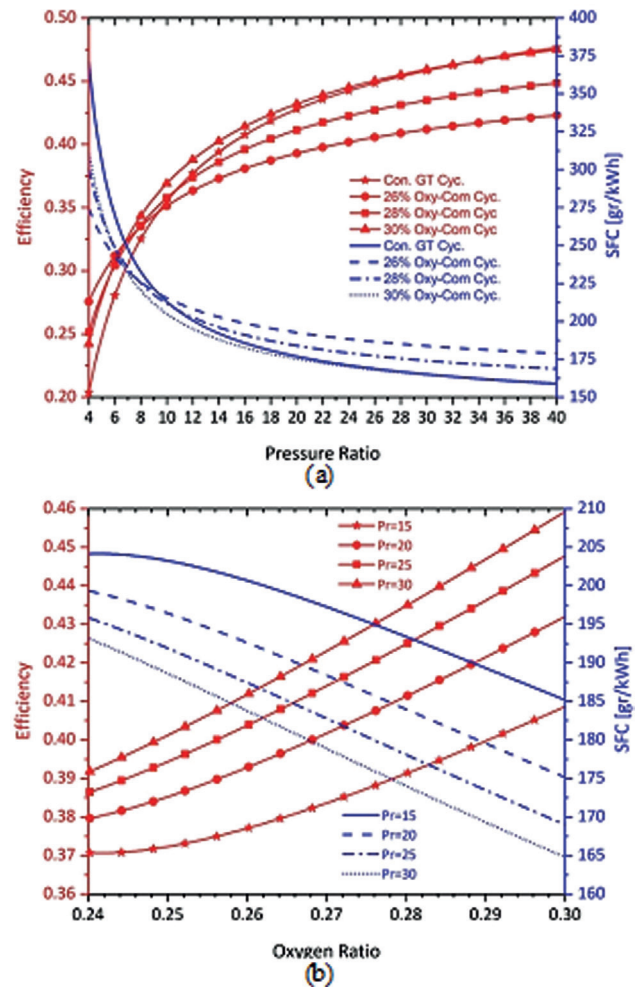


Figure 3. (a) Change of heat added and net power with pressure ratio for various oxygen fractions, (b) Change of heat added and net power with oxygen ratio for various pressure ratio.

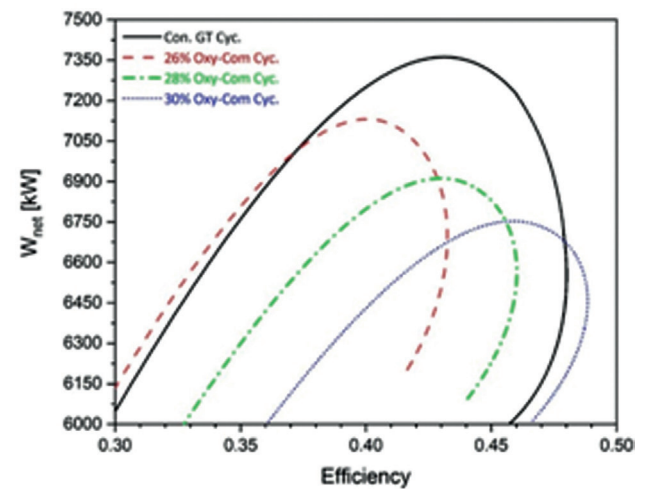
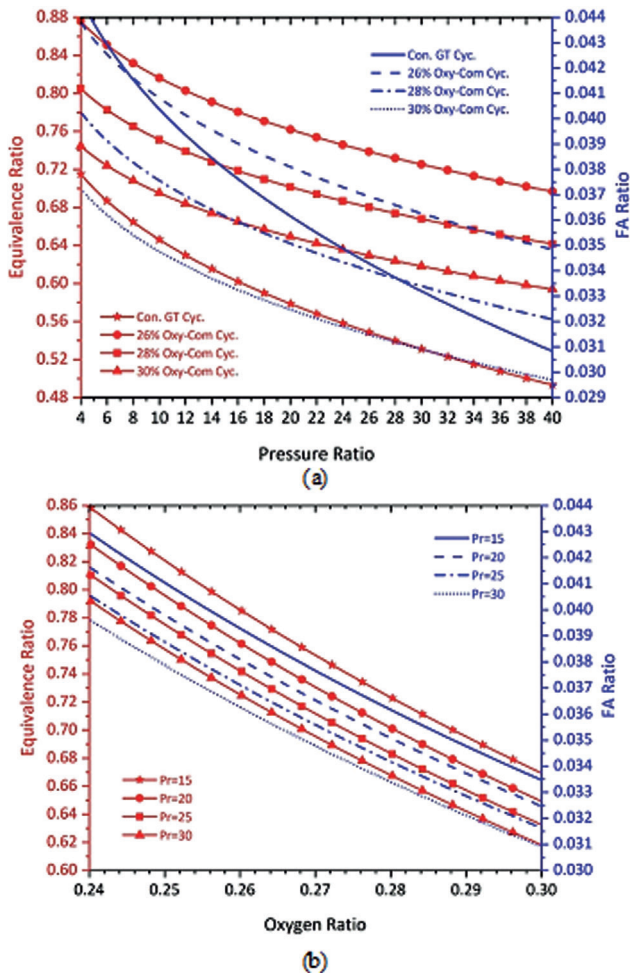


Figure 4. Change of net power and efficiency with pressure ratio for various oxygen fractions.

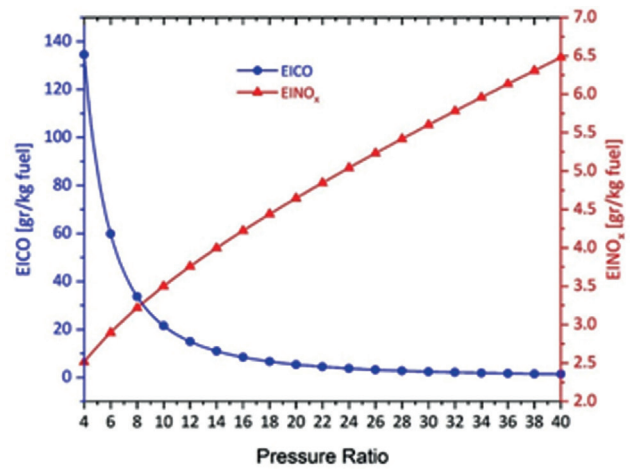




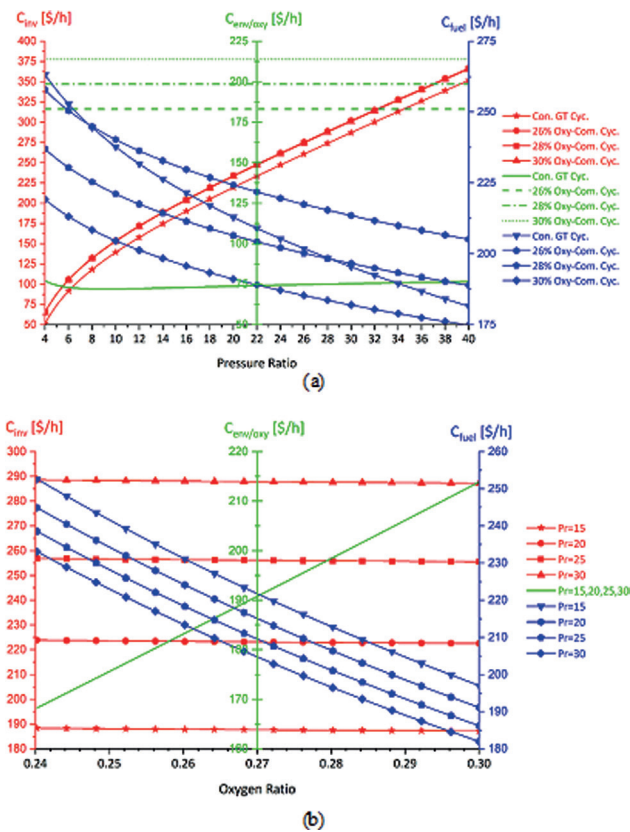
**Figure 5.** (a) Change of equivalence ratio and FA ratio with pressure ratio for various oxygen fractions, (b) Change of equivalence ratio and FA ratio with oxygen ratio for various pressure ratio.

and oxy-combustion power systems, the equivalence ratio decreases. The equivalence ratio decrease is greater in conventional gas turbine power systems than in oxy-combustion power systems. A decrease in the equivalence ratio causes lower fuel consumption for the constant working fluid. Similarly, the FA ratio decreases with increases in the pressure ratio. For oxy-combustion power systems, the FA ratio is calculated using the oxidant that provides combustion instead of air. While a parallel exists in the decrease in the FA ratio in oxy-combustion power systems, the conventional gas turbine power systems' slope for the FA ratio decrease is greater. Figure 5b shows increases in the oxygen ratio to steadily decrease both the FA and equivalence ratios. No significant difference has been found when increasing the pressure ratio from 15 to 30.

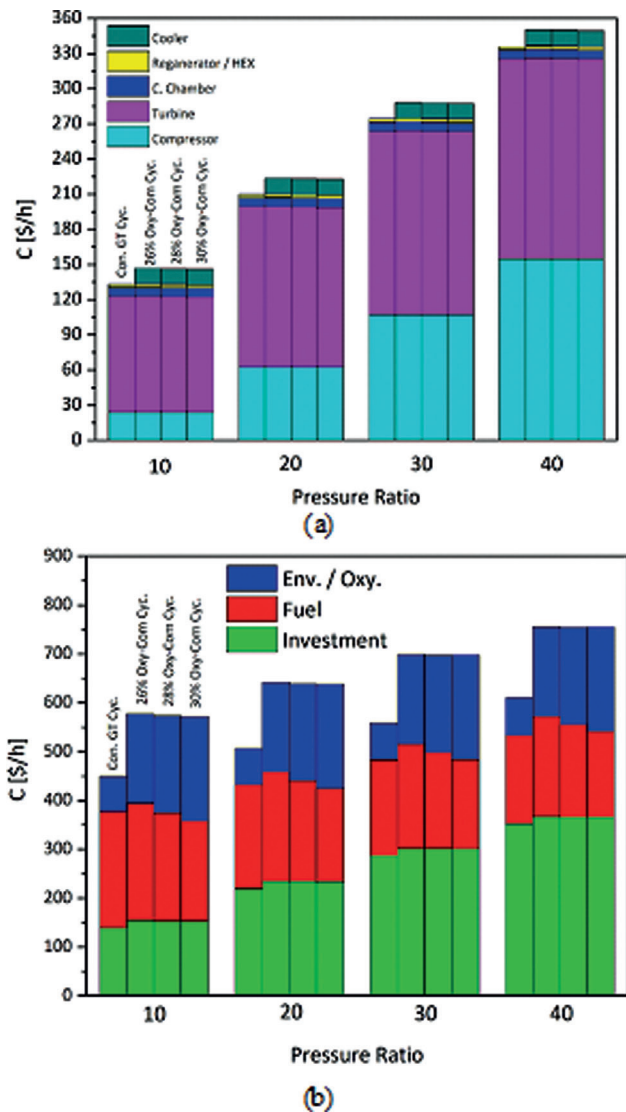
Figure 6 shows  $\text{NO}_x$  and CO emissions per kg of fuel with respect to the pressure ratio for the conventional



**Figure 6.** Change of  $\text{EINO}_x$  and EICO with pressure ratio for conventional gas turbine power cycle.

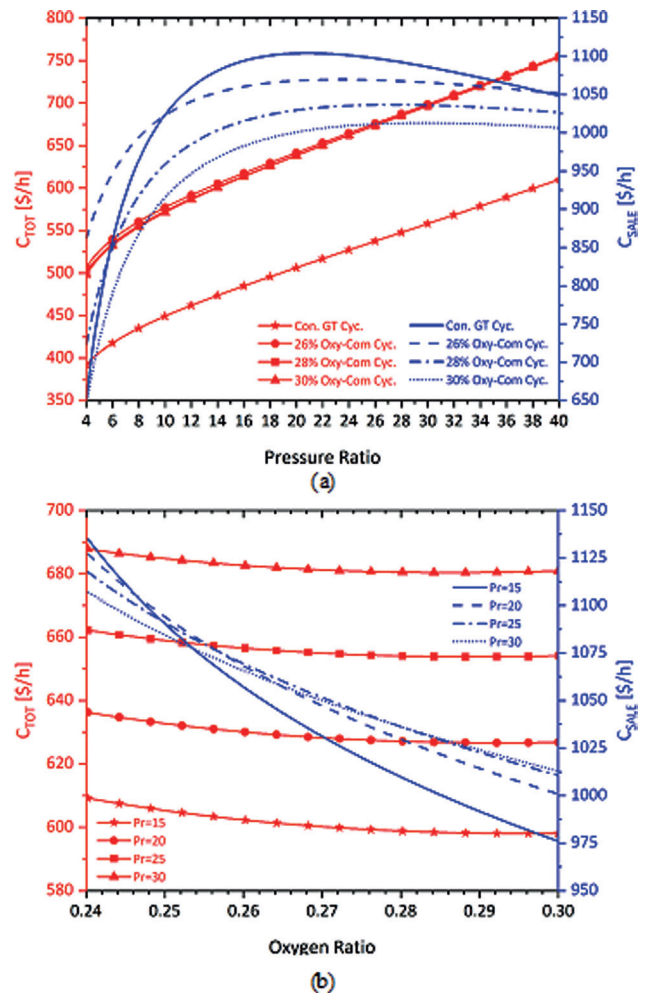


**Figure 7.** (a) Change of capital investment cost, environmental/oxygen cost and fuel cost with pressure ratio for various oxygen fractions, (b) Change of capital investment cost, environmental/oxygen cost and fuel cost with oxygen ratio for various pressure ratio.



**Figure 8.** (a) Effect of pressure ratio and oxygen ratio on capital investment with different system components cost. (b) Effect of pressure ratio and oxygen ratio on total cost with different investment, fuel, and environmental/oxygen costs.

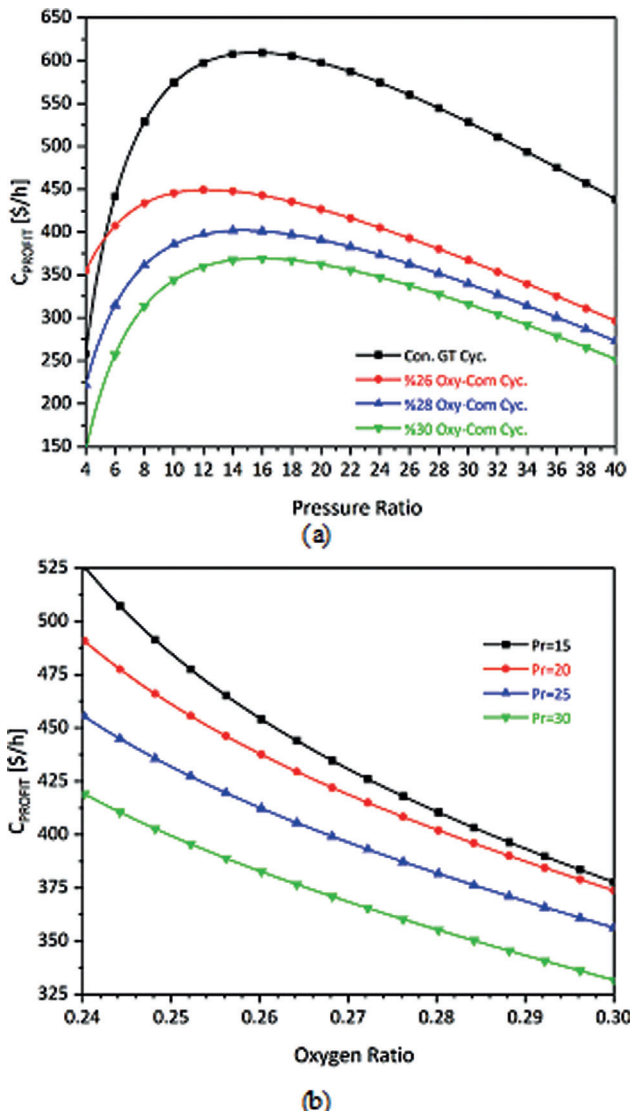
gas turbine power system. Oxy-combustion power cycles appear to be a green energy system. Oxy-combustion power cycles prevent the release of harmful emissions such as  $\text{NO}_x$  and  $\text{CO}$  into the environment. In addition, the  $\text{H}_2\text{O}$  released after combustion is separated using a water separator. The release of highly harmful global-warming emissions such as  $\text{CO}_2$  is prevented by storing it within oxy-combustion power systems. Assuming that approximately 2.45 kg of  $\text{CO}_2$  [40,41] is produced per kg of natural gas, how important using oxy-combustion power systems is for producing energy without harming the environment can be seen. Economic costs can be recovered in the future; however,



**Figure 9.** (a) Change of total cost and sale cost with pressure ratio for various oxygen fractions, (b) Change of total cost and sale cost with oxygen ratio for various pressure ratio.

the environmental damage is something from which the world cannot recover. For this reason, the importance of oxy-combustion power systems will increase in the search for zero-emission systems with the new harmful emission penalty rules that will come into effect in the coming years.

Figures 7a and 7b show the effect various pressure and oxygen ratios have on capital investment cost, environmental/oxygen cost, and fuel cost. Figure 7a shows capital investment costs to increase as the pressure ratio increases. The components common to the conventional gas turbine power system and oxy-combustion power system are the compressor, regenerator, combustion chamber, and turbine. Oxy-combustion power systems have a difference in the capital investment cost due to the use of a cooler. When examined with respect to the pressure ratio, the total emission costs ( $\text{NO}_x$ ,  $\text{CO}$ , and  $\text{CO}_2$ ) continue to increase slightly after the initial decrease because the  $\text{NO}_x$  and  $\text{CO}$  formations



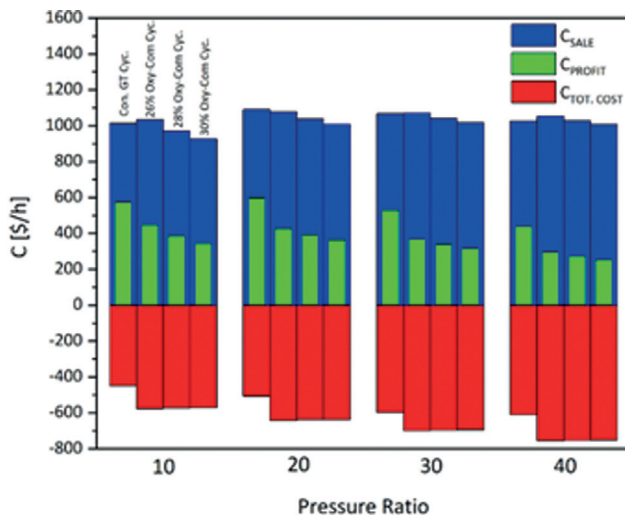
**Figure 10.** (a) Change of total profit with pressure ratio for various oxygen fractions, (b) Change of total profit with oxygen ratio for various pressure ratio.

have opposing ratios, as shown in Figure 6. In the fuel cost analysis, fuel consumption decreases with increases in the pressure ratio when keeping the turbine inlet temperature constant. Fuel consumption in conventional gas turbine power systems is higher than in oxy-combustion power systems. However, this result changes as the pressure ratio increases. Only the 30% oxy-combustion power cycle has consistently lower fuel costs than conventional gas turbine power cycles. Figure 7b shows the capital investment cost to remain constant while increases in the oxygen ratio increase the investment cost. In addition, increasing the pressure ratio from 15 to 30 does not change the oxygen cost. In addition, fuel costs decrease with increases in both the oxygen and pressure ratios in oxy-combustion power

cycles. Figure 8a shows the capital investment costs for the system components at four different pressure ratios. Increases in the pressure ratio result in almost no change in cost for the combustion chamber, regenerator/regenerative heat exchanger, or cooler, while considerably increasing the costs for the compressors and turbines. As the pressure ratio increases, the number of blades and stages increase, and due to the high cost of compressor and turbine blades, their investment costs increase dramatically. Figure 8b shows the total cost for the components of power systems at four different pressure ratios, thus showing how the investment, fuel, environment, and oxygen costs affect the total cost of the system.

Figures 9a and 9b show the effect changes in the pressure and oxygen ratios have on total cost and electricity revenue. Figure 9a shows total costs to decreasing with increases in the oxygen ratio from 26% to 30% in oxy-combustion power systems. These values practically balance each other out in the total cost calculation. Thus, the total cost is almost the same for each of the oxy-combustion power cycles at the three different oxygen ratios. In addition, the total cost of a conventional gas turbine power cycle is on average \$150 per hour less expensive than oxy-combustion power cycles. Electricity revenue is related to the net power obtained from the systems. The more power that is obtained, the more that is gained from electricity revenue. Therefore, Figures 9a and 9b show revenue to be related to net power. Increasing the pressure and oxygen ratios have the same effect. The total cost decreases slightly as the rate of oxygen increases. In oxy-combustion power cycles, the total cost increases as the pressure ratio increases from 15 to 30.

Figures 10a and 10b show the effect that variations in the pressure and oxygen ratios have on net profit. Net profit is obtained when the total cost is subtracted from the electricity revenue. The most important result from an economic system analysis is net profit. System selection is made according to the profit obtained because net profit is calculated using many parameters. Net profit is calculated using costs for power, efficiency, equivalence/FA ratio and fuel consumption, capital investment of the system components, and fuel/environment/oxygen. According to the results, the net profit for the conventional gas turbine power cycle increases rapidly up to a pressure ratio of 15.9 and then decreases. For the oxy-combustion power cycles with 26%, 28% and 30% oxygen ratios, net profit peaks at 12.8, 15.2, and 16.4 pressure ratios, respectively. Figure 10a shows the maximum and optimum points with the pink line. As a result, the maximum net power occurs at the 20.8, 23.3, 27.4, and 29.7 pressure ratios, respectively when examining the system thermo-economically, while the points of optimum profit vary. When performing a system performance analysis, analyzing a system only in terms of energy may give incorrect or incomplete results when studying of power cycles. Therefore, energy, environmental, and economic aspects should be fully considered. As can



**Figure 11.** Effect of pressure ratio and oxygen ratio on total cost, sale cost and total profit.

be seen, Figure 11 displays the revenue, total cost, and net profit results obtained for the 10, 20, 30, and 40 pressure ratios for the power cycles. Thus, all economic results are shown when comparing the systems. Before constructing a power plant, these figures should be drawn at the optimum pressure ratio with respect to what is desired to be selected while considering all the parameters and factors.

## CONCLUSION

In this study, the thermodynamic analyses of the conventional gas turbine power cycle and environmentally promising oxy combustion power cycle are done. In thermodynamic analyses, energy, environment and economic aspects are examined in detail. Parametric analyses results are obtained for pressure ratios from 4 to 40 and oxygen ratios ranging from 24% to 30%.

- With the increase in the pressure ratio, the net power increased rapidly in both the conventional gas turbine power cycle and the oxy combustion power cycles, and after reaching a peak, it decreases slightly. The pressure ratio at maximum net power is 20.8 for conventional gas turbine power cycle. The peak points in oxy-combustion power cycles with 26%, 28% and 30% oxygen ratio are 23.3, 27.4 and 29.7, respectively. The net power output decreased with increasing oxygen ratios. The heat added in all cycles decreased with the increase of both the pressure ratios and the oxygen ratios.
- System efficiencies increased with both the pressure ratios and the oxygen ratios increased, since the increase net power is greater than the increase

in heat addition. On the other hand, the specific fuel consumption decreased with increasing the pressure ratios and the oxygen ratios.

- With increasing the pressure ratios and the oxygen ratios, the corresponding equivalence ratios and the fuel-air ratios decreased for a constant working fluid.
- Using oxy-combustion cycles less  $\text{NO}_x$  and CO emissions released, around 3-6.5 g/kg fuel and 2-135 g/kg fuel, respectively. On the other hand, in oxy-combustion pure oxygen instead of air, resulting increase in costs by 183 \$/h, 198 \$/h and 213 \$/h, respectively for %26, %28 ve %30 oxygen ratios.
- The increase in the pressure ratios increased the capital investment cost of the facility, while the increase in the oxygen ratios is not affected. Increasing the pressure ratios and the oxygen ratios reduced the fuel cost of the system for the constant working fluid.
- It is concluded that, the total cost of conventional gas turbine power cycle is less than the oxy-combustion power cycle. Also, it has been seen in the most profitable system in terms of net profit. Because the electricity revenue of the conventional gas turbine power cycle is greater than the oxy-combustion power cycle.
- Although the total cost in oxy-combustion power cycles is almost equal, the resulting electricity revenues are greater than the rest in oxy-combustion with 26% oxygen. As a result, in terms of total profit power cycles with oxy-combustion systems can be arranged from highest to lowest with 26%, 28% and 30% oxygen ratios, respectively.
- System component costs, investment/fuel/environment/oxygen costs, total cost, revenue and net profit results were presented for all power cycles at four different pressure ratios (10, 20, 30 and 40).

Oxy-combustion power cycles have higher cost compared to conventional gas turbine power cycles currently. However, it will become more popular due to the decreasing cost of pure oxygen with the developing technologies and increasing environmental sensitivities in the following years. Advanced technology systems studies will be carried out with economic oxygen production systems.

## ACKNOWLEDGEMENT

This work is compiled from the first author's unpublished Ph.D. dissertation. We would like to thank the Turkish Academy of Sciences (TUBA-GEBIP) and The Scientific and Technological Research Council of Turkey (TUBITAK) for their support for graduate students.

## NOMENCLATURE

- |     |   |
|-----|---|
| $a$ | mole number of reactant O <sub>2</sub>  |
| $b$ | mole number of reactant CO <sub>2</sub> |

<i>c</i>	mole number of reactant N <sub>2</sub>
<i>C</i>	cost
<i>CC</i>	combustion chamber
<i>E</i>	energy
<i>FA</i>	fuel/air ratio
<i>h</i>	specific enthalpy (kJ/kg)
<i>LHV</i>	lower heat value
<i>N</i>	total number of moles of species
<i>NG</i>	natural gas
<i>OEM</i>	original equipment manufacturer
<i>Pr</i>	pressure ratio
<i>s</i>	specific entropy (kJ/kg K)
<i>SFC</i>	specific fuel consumption
<i>T</i>	temperature (K)
<i>V</i>	volume
<i>X</i>	total number of carbon atom
<i>Y</i>	total number of hydrogen atoms
<i>Z</i>	total number of oxygen atoms
<i>Q</i>	total number of nitrogen atoms
<i>W</i>	power

## Greek symbols

$\alpha$	mole fraction
$\varepsilon$	molar air-fuel ratio
$\Phi$	equivalence ratio
$\chi$	number of moles of exhaust species

## Subscripts

<i>a</i>	air
<i>ady</i>	adiabatic
<i>c</i>	compressor
<i>cc</i>	combustion chamber
<i>env</i>	environmental
<i>f</i>	fuel
<i>fu</i>	fluid or oxidant
<i>in</i>	inlet
<i>inv</i>	investment
<i>k</i>	exhaust species
<i>net</i>	net
<i>p</i>	pressure
<i>pz</i>	primary zone
<i>r</i>	reactants
<i>ox</i>	oxidant
<i>oxy</i>	oxygen
<i>s</i>	stoichiometric
<i>wf</i>	working fluid
<i>t</i>	turbine
<i>x</i>	number of carbon atoms
<i>y</i>	number of hydrogen atoms
<i>z</i>	number of oxygen atoms
<i>q</i>	number of nitrogen atoms

## AUTHORSHIP CONTRIBUTIONS

Authors equally contributed to this work.

## DATA AVAILABILITY STATEMENT

The authors confirm that the data that supports the findings of this study are available within the article. Raw data that support the finding of this study are available from the corresponding author, upon reasonable request.

## CONFLICT OF INTEREST

The author declared no potential conflicts of interest with respect to the research, authorship, and/or publication of this article.

## ETHICS

There are no ethical issues with the publication of this manuscript.

## REFERENCES

- [1] Mletzko J, Ehlers S, Kather A. Comparison of Natural gas combined cycle power plants with post combustion and oxyfuel technology at different CO<sub>2</sub> capture rates. *Energy Proced* 2016;86:2–11. [\[CrossRef\]](#)
- [2] Ferrari N, Mancuso L, Davison J, Chiesa P, Martelli E, Romano MC. Oxy-turbine for Power Plant with CO<sub>2</sub> Capture. *Energy Proced* 2017;114:471–480. [\[CrossRef\]](#)
- [3] Climent Barba F, Martínez-Denegri Sánchez G, Soler Seguí B, Gohari Darabkhani H, Anthony EJ. A technical evaluation, performance analysis and risk assessment of multiple novel oxy-turbine power cycles with complete CO<sub>2</sub> capture. *J Clean Prod* 2016;133:971–985. [\[CrossRef\]](#)
- [4] Xiang Y, Cai L, Guan Y, Liu W, Han Y, Liang Y. Study on the configuration of bottom cycle in natural gas combined cycle power plants integrated with oxy-fuel combustion. *Appl Energy* 2018;212:465–477. [\[CrossRef\]](#)
- [5] Gładysz P, Stanek W, Czarnowska L, Węcel G, Langørgen Ø. Thermodynamic assessment of an integrated MILD oxyfuel combustion power plant. *Energy* 2017;137:761–774. [\[CrossRef\]](#)
- [6] Gładysz P, Ziębik A. Life cycle assessment of an integrated oxy-fuel combustion power plant with CO<sub>2</sub> capture, transport and storage - Poland case study. *Energy* 2015;92:328–340. [\[CrossRef\]](#)
- [7] Liu M, Lior N, Zhang N, Han W. Thermoeconomic Optimization of Coolcep-s: a Novel Zero-CO<sub>2</sub> Emission Power Cycle Using LNG (Liquified Natural Gas) Coldness. 2008 ASME International Mechanical Engineering Congress and Exposition 2008;8:847–858. [\[CrossRef\]](#)
- [8] Farooqui A, Bose A, Ferrero D, Llorca J, Santarelli M. Techno-economic and exergetic assessment of an oxy-fuel power plant fueled by syngas produced by

- chemical looping CO<sub>2</sub> and H<sub>2</sub>O dissociation. *J CO<sub>2</sub> Util* 2018;27:500–517. [\[CrossRef\]](#)
- [9] Ziółkowski P, Zakrzewski W, Kaczmarczyk O, Badur J. Thermodynamic analysis of the double Brayton cycle with the use of oxy combustion and capture of CO<sub>2</sub>. *Arch Thermodyn* 2013;34:23–38. [\[CrossRef\]](#)
- [10] Liu CY, Chen G, Sipöcz N, Assadi M, Bai XS. Characteristics of oxy-fuel combustion in gas turbines. *Appl Energy* 2012;89:387–394. [\[CrossRef\]](#)
- [11] Guan Y, Han Y, Wu M, Liu W, Cai L, Yang Y, et al. Simulation study on the carbon capture system applying LNG cold energy to the O<sub>2</sub>/H<sub>2</sub>O oxy-fuel combustion. *Natural Gas Industry B* 2018;5:270–275. [\[CrossRef\]](#)
- [12] Han SH, Lee YS, Cho JR, Lee KH. Efficiency analysis of air-fuel and oxy-fuel combustion in a reheating furnace. *Int J Heat Mass Transf* 2018;121:1364–1370. [\[CrossRef\]](#)
- [13] Shakeel MR, Sanusi YS, Mokheimer EMA. Numerical modeling of oxy-methane combustion in a model gas turbine combustor. *Appl Energy* 2018;228:68–81. [\[CrossRef\]](#)
- [14] Mehrpooya M, Zonouz MJ. Analysis of an integrated cryogenic air separation unit, oxy-combustion carbon dioxide power cycle and liquefied natural gas regasification process by exergoeconomic method. *Energy Convers Manag* 2017;139:245–259. [\[CrossRef\]](#)
- [15] Mehrpooya M, Sharifzadeh MMM, Katooli MH. Thermodynamic analysis of integrated LNG regasification process configurations. *Progress Energy Combust Sci* 2018;69:1–27. [\[CrossRef\]](#)
- [16] Mehrpooya M, Ansarinassab H, Sharifzadeh MMM, Rosen MA. Conventional and advanced exergoeconomic assessments of a new air separation unit integrated with a carbon dioxide electrical power cycle and a liquefied natural gas regasification unit. *Energy Convers Manag* 2018;163:151–168. [\[CrossRef\]](#)
- [17] Mehrpooya M, Ghorbani B. Introducing a hybrid oxy-fuel power generation and natural gas/ carbon dioxide liquefaction process with thermodynamic and economic analysis. *J Clean Prod* 2018;204:1016–10133. [\[CrossRef\]](#)
- [18] Hong J, Field R, Gazzino M, Ghoniem AF. Operating pressure dependence of the pressurized oxy-fuel combustion power cycle. *Energy* 2010;35:5391–5399. [\[CrossRef\]](#)
- [19] Oki Y, Hamada H, Kobayashi M, Yuri I, Hara S. Development of High-efficiency Oxy-fuel IGCC System. *Energy Proced* 2017;114:501–504. [\[CrossRef\]](#)
- [20] Esquivel-Patiño GG, Serna-González M, Nápoles-Rivera F. Thermal integration of natural gas combined cycle power plants with CO<sub>2</sub> capture systems and organic Rankine cycles. *Energy Convers Manag* 2017;151:334–342. [\[CrossRef\]](#)
- [21] Ez Abadi AM, Sadi M, Farzaneh-Gord M, Ahmadi MH, Kumar R, Chau K. A numerical and experimental study on the energy efficiency of a regenerative Heat and Mass Exchanger utilizing the counter-flow Maisotsenko cycle. *Eng Appl Comput Fluid* 2020;14:1–12. [\[CrossRef\]](#)
- [22] Ramezanizadeh M, Alhuyi Nazari M, Ahmadi MH, Chau K. Experimental and numerical analysis of a nanofluidic thermosyphon heat exchanger. *Eng Appl Comput Fluid* 2019;13:40–47. [\[CrossRef\]](#)
- [23] Akbarian E, Najafi B, Jafari M, Faizollahzadeh Ardabili S, Shamshirband S, Chau K. Experimental and computational fluid dynamics-based numerical simulation of using natural gas in a dual-fueled diesel engine. *Eng Appl Comput Fluid Mech* 2018;12:517–534. [\[CrossRef\]](#)
- [24] Baghban A, Sasanipour J, Pourfayaz F, Ahmadi MH, Kasaeian A, Chamkha AJ, et al. Towards experimental and modeling study of heat transfer performance of water- SiO<sub>2</sub> nanofluid in quadrangular cross-section channels. *Eng Appl Comput Fluid Mech* 2019;13:453–469. [\[CrossRef\]](#)
- [25] Ghalandari M, Mirzadeh Koohshahi E, Mohamadian F, Shamshirband S, Chau KW. Numerical simulation of nanofluid flow inside a root canal. *Eng Appl Comput Fluid Mech* 2019;13:254–264. [\[CrossRef\]](#)
- [26] Ozsari I, Ust Y. Effect of varying fuel types on oxy-combustion performance. *Int J Energy Res* 2019;43:8684–8696. [\[CrossRef\]](#)
- [27] Scaccabarozzi R, Gatti M, Martelli E. Thermodynamic analysis and numerical optimization of the NET Power oxy-combustion cycle. *Appl Energy* 2016;178:505–526. [\[CrossRef\]](#)
- [28] Thorbergsson E, Grönstedt T. A Thermodynamic analysis of two competing mid-sized oxyfuel combustion combined cycles. *J Energy* 2016;2016:1–14. [\[CrossRef\]](#)
- [29] Khallaghi N, Hanak DP, Manovic V. Staged oxy-fuel natural gas combined cycle. *Appl Therm Eng* 2019;153:761–767. [\[CrossRef\]](#)
- [30] Kotowicz J, Michalski S, Brzeczek M. The characteristics of a modern oxy-fuel power plant. *Energies* 2019;12:3374. [\[CrossRef\]](#)
- [31] Shan S, Zhou Z, Cen K. An innovative integrated system concept between oxy-fuel thermo-photovoltaic device and a Brayton-Rankine combined cycle and its preliminary thermodynamic analysis. *Energy Convers Manag* 2019;180:1139–1152. [\[CrossRef\]](#)
- [32] Son S, Heo JY, Kim NI, Jamal A, Lee JI. Reduction of CO<sub>2</sub> emission for solar power backup by direct integration of oxy-combustion supercritical CO<sub>2</sub> power cycle with concentrated solar power. *Energy Convers Manag* 2019;201:112161. [\[CrossRef\]](#)

- [33] Tahir F, Ali H, Baloch AAB, Jamil Y. Performance analysis of air and oxy-fuel laminar combustion in a porous plate reactor. *Energies* 2019;12:1706. [CrossRef]
- [34] Habib MA, Imteyaz B, Nemitallah MA. Second law analysis of premixed and non-premixed oxy-fuel combustion cycles utilizing oxygen separation membranes. *Appl Energy* 2020;259:114213. [CrossRef]
- [35] Wimmer K, Sanz W. Optimization and comparison of the two promising oxy-combustion cycles NET power cycle and graz cycle. *Int J Greenhouse Gas Control* 2020;99:103055. [CrossRef]
- [36] Demirbas A. *Methane Gas Hydrate*. London: Springer; 2010. [CrossRef]
- [37] Agentschap Telecom Ministerie Van Economische Zaken. *Gas Composition Transition Agency Report 2013*. Berlin: Agentschap Telecom Ministerie Van Economische Zaken; 2013.
- [38] Barzegar Avval H, Ahmadi P, Ghaffarizadeh AR, Saidi MH. Thermo-economic-environmental multi-objective optimization of a gas turbine power plant with preheater using evolutionary algorithm. *Int J Energy Res* 2011;35:389–403. [CrossRef]
- [39] Kayadelen HK, Ust Y. Thermodynamic, environmental and economic performance optimization of simple, regenerative, STIG and RSTIG gas turbine cycles. *Energy* 2017;121:751–771. [CrossRef]
- [40] Ramstein C, Dominioni G, Ettehad S, Lam L, Quant M, Zhang J, et al. *State and Trends of Carbon Pricing 2019*. Washington: The World Bank; 2019.
- [41] International Energy Agency. *Oxy-Combustion Turbine Power Plant*. International Energy Agency Report. Report No: 2015/05. Paris: International Energy Agency; 2015.
- [42] Portillo E, Alonso-Fariñas B, Vega F, Cano M, Navarrete B. Alternatives for oxygen-selective membrane systems and their integration into the oxy-fuel combustion process: A review. *Sep Purif Technol* 2019;229:115708. [CrossRef]
- [43] Ebrahimi A, Meratizaman M, Akbarpour Reyhani H, Pourali O, Amidpour M. Energetic, exergetic and economic assessment of oxygen production from two columns cryogenic air separation unit. *Energy* 2015;90:1298–1316. [CrossRef]
- [44] Lefebvre AH, Ballal DR. *Gas turbine combustion alternative fuels and emissions*. Boca Raton: Taylor & Francis; 2010. [CrossRef]
- [45] Lieuwen TC, Yang V, editors. *Gas Turbine Emissions*. Cambridge: Cambridge University Press; 2013. [CrossRef]
- [46] Geo AR. *New Developments in Combustion Technology—Part II: Step Change in Efficiency 2012*. National Energy Technology Laboratory.
- [47] Ferguson CR. *Internal Combustion Engines – Applied Thermosciences*. New York: John Wiley&Sons Inc.; 1986.
- [48] Ozsari I, Ust Y, Kayadelen HK. Comparative energy and emission analysis of oxy-combustion and conventional air combustion. *Arab J Sci Eng* 2021;46:2477–2492. [CrossRef]
- [49] Turns SR. *An introduction to combustion: concepts and applications*. 3. ed. Boston: McGraw-Hill; 2011.
- [50] Seyyedi SM, Ajam H, Farahat S. Thermoenviromonic optimization of gas turbine cycles with air preheat. *Proceed of the Inst Mech Eng Part A J Power and Energy* 2011;225:12–23. [CrossRef]
- [51] Lazzaretto A, Toffolo A. Energy, economy and environment as objectives in multi-criterion optimization of thermal systems design. *Energy* 2004;29:1139–1157. [CrossRef]
- [52] Sayyaadi H. Multi-objective approach in thermoenviromonic optimization of a benchmark cogeneration system. *Appl Energy* 2009;86:867–879. [CrossRef]
- [53] Dincer I, Rosen M. *Exergy: Energy, Environment and Sustainable Development*. 2. ed. Amsterdam: Elsevier; 2013. [CrossRef]
- [54] Kayadelen HK, Ust Y. Performance and environment as objectives in multi-criterion optimization of steam injected gas turbine cycles. *Appl Therm Eng* 2014;71:184–196. [CrossRef]
- [55] Rizk NK, Mongia HC. Semianalytical correlations for NO<sub>x</sub>, CO, and UHC emissions. *J Eng Gas Turbines Power* 1993;115:612–619. [CrossRef]
- [56] Valero A, Lozano MA, Serra L, Tsatsaronis G, Pisa J, Frangopoulos C, et al. CGAM problem: Definition and conventional solution. *Energy* 1994;19:279–286. [CrossRef]
- [57] Oyedepo SO, Fagbenle RO, Adefila SS, Alam M, Pham D. Exergy costing analysis and performance evaluation of selected gas turbine power plants. *Cogent Eng* 2015;2:1101048. [CrossRef]
- [58] Ahmadi P, Dincer I. Thermodynamic analysis and thermoeconomic optimization of a dual pressure combined cycle power plant with a supplementary firing unit. *Energy Convers Manag* 2011;52:2296–2308. [CrossRef]
- [59] Roosen P, Uhlenbruck S, Lucas K. Pareto optimization of a combined cycle power system as a decision support tool for trading off investment vs. operating costs. *Int J Therm Sci* 2003;42:553–560. [CrossRef]
- [60] Frangopoulos CA. Application of the thermoeconomic functional approach to the CGAM problem. *Energy* 1994;19:323–342. [CrossRef]